Quantitative Phase-Field Approach for Simulating Grain Growth in Anisotropic Systems with Arbitrary Inclination and Misorientation Dependence

N. Moelans,[*] B. Blanpain, and P. Wollants

Department of Metallurgy and Materials Engineering, Katholieke Universiteit Leuven,
Kasteelpark Arenberg 44, bus 2450, 3001 Leuven, Belgium
(Received 9 February 2008; published 10 July 2008)

A phase-field approach for quantitative simulations of grain growth in anisotropic systems is introduced, together with a new methodology to derive appropriate model parameters that reproduce given misorientation and inclination dependent grain boundary energy and mobility in the simulations. The proposed model formulation and parameter choice guarantee a constant diffuse interface width and consequently give high controllability of the accuracy in grain growth simulations.

The phase-field method has a reputation to be very general and applicable to complex microstructural phenomena. Besides many other applications, it has proven to be extremely suitable for the study of grain growth related phenomena in 2D [1–3] and 3D [4–6]. For given grain boundary energy and mobility, the simulations predict the evolution of a grain structure and its macroscopic parameters, such as the grain size and grain orientation distributions [7]. It is, however, still a great challenge to derive reliable quantitative conclusions from the simulations, especially for anisotropic systems. Atomistic molecular dynamics studies have recently shown that grain boundary properties vary considerably with misorientation and boundary inclination [8,9]. Furthermore, important mesoscale processes, such as recrystallazition and abnormal grain growth, are controlled by these variations in grain boundary properties [10–12]. An improved phase-field formulation for grain growth is thus required.

Generally, three phase-field approaches exist for simulating the evolution of anisotropic polycrystalline structures. In the Warren, Kobayashi, and Carter approach [13], 3 continuous orientation fields, or 4 quaternions [14], are used to represent variations in local orientation, in combination with a phase field, representing the local crystallinity. The free energy functional is formulated so that it results in a Read-Shockley dependence of the grain boundary energy at low misorientations. This model has been applied to polycrystalline solidification [15] and for the study of structural transitions for stationary grain boundaries [16]. It is, however, less suitable for long-term coarsening [17]. Furthermore, little attention has been given to grain boundary energies with cusps at high-angle misorientations. In the multiphase-field [5,18] and continuum-field approach [1,2], different grain orientations are represented by a large set of phase fields. In the multiphase-field approach, the phase-field variables are interpreted as fractions for which the sum equals 1 at each position. In principle, the model can treat arbitrary misorientation and inclination dependence. There exist straightforward

relations between the model parameters and grain boundary energy and mobility for 2-grain structures. For multigrain structures, however, extra phase fields (other than those representing the neighboring grains), so-called ''ghost'' fields, contribute at grain boundaries. Consequently, it is difficult to control the grain boundary properties in a quantitative way. The ghost fields may be suppressed by using alternative free energy functionals [19,20], however, not completely and for arbitrarily large variations in grain boundary energy. In the continuum-field approach, there is no restriction on the local values of the phase fields, which makes it more easy to avoid ghost fields at interfaces. Moreover, different from the other models, the inclination dependence of the grain boundary energy is introduced through both the homogeneous and gradient contributions in the free energy functional [2,21]. This degree of freedom can be used to keep the diffuse grain boundary width constant for varying grain boundary properties, as variations in grain boundary width are inefficient from a computational point of view and might introduce nonphysical effects [22]. (In phase-field simulations for grain growth, the grain boundary width is usually treated as a model parameter and chosen based on computational considerations, a so-called ''thin-interface'' approach.) However, the proposed methodology to determine the model parameters is very approximate. They assume that the diffuse grain boundary width is proportional with $\sqrt{1/(\Delta f)_{max}}$ and grain boundary energy with $\sqrt{(\Delta f)_{max}}$, where $(\Delta f)_{max}$ is defined as ''the maximum height of the barrier in the homogeneous free energy f between two degenerate minima,'' although it is not specified how this value is related to the model parameters. In fact, as we show in this Letter and in more detail in [23], the grain boundary energy and thickness are related to the free energy density in a more complicated way. It is also not described how to treat faceted boundaries.

The purpose of this Letter is to introduce a fully quantitative phase-field approach for polycrystalline structures with arbitrary anisotropy, and give a procedure to deter-

mine its model parameters. We start from the continuum-field formulation of Kazaryan *et al.* [2,21]. A grain structure is represented by a large set of independent phase fields $\eta_1(\mathbf{r}, t)$, $\eta_2(\mathbf{r}, t)$, ..., $\eta_i(\mathbf{r}, t)$, ... $\eta_p(\mathbf{r}, t)$. Their evolution is given by Ginzburg-Landau equations:

$$\frac{\partial \eta_i(\mathbf{r}, t)}{\partial t} = -L(\theta, \phi) \frac{\delta F(\eta_1, \eta_2, \ldots, \eta_p)}{\delta \eta_i(\mathbf{r}, t)}, \quad (1)$$

where we propose a free energy functional F

$$F = \int_V \left[m f_0(\eta_1, \ldots, \eta_p) + \frac{\kappa(\theta, \phi)}{2} \sum_{i=1}^p (\nabla \eta_i)^2 \right] dV, \quad (2)$$

with

$$f_0(\eta_1, \ldots, \eta_p) = \sum_{i=1}^p \left(\frac{\eta_i^4}{4} - \frac{\eta_i^2}{2} \right) + \sum_{i=1}^p \sum_{j>i}^p \gamma(\theta, \phi) \eta_i^2 \eta_j^2 + \frac{1}{4}. \quad (3)$$

For $\gamma > 0.5$, f_0 has localized minima at $(\eta_1, \ldots, \eta_p) = (1, 0, \ldots, 0), (0, 1, 0, \ldots, 0), \ldots, (0, \ldots, 0, 1)$, representing discrete grain orientations (we only consider positive values of the phase fields). Because of the cross products, ghost fields always result in an increase of the local free energy and are accordingly unstable. Therefore, expressions for the grain boundary properties derived for 2-grain structures remain valid for individual grain boundaries in polycrystalline structures, except for very small grains. The kinetic parameter L and the parameters κ and γ in the free energy are a function of the misorientation θ between neighboring grains and the grain boundary inclination ϕ:

$$\kappa(\theta, \phi) = \frac{\sum_{i=1}^p \sum_{j>i}^p \kappa_{i,j}(\phi_{i,j}) \eta_i^2 \eta_j^2}{\sum_{i=1}^p \sum_{j>i}^p \eta_i^2 \eta_j^2}, \quad (4a)$$

$$\gamma(\theta, \phi) = \frac{\sum_{i=1}^p \sum_{j>i}^p \gamma_{i,j}(\phi_{i,j}) \eta_i^2 \eta_j^2}{\sum_{i=1}^p \sum_{j>i}^p \eta_i^2 \eta_j^2}, \quad (4b)$$

$$L(\theta, \phi) = \frac{\sum_{i=1}^p \sum_{j>i}^p L_{i,j}(\phi_{i,j}) \eta_i^2 \eta_j^2}{\sum_{i=1}^p \sum_{j>i}^p \eta_i^2 \eta_j^2}, \quad (4c)$$

with

$$\phi_{i,j} = \frac{\nabla \eta_i - \nabla \eta_j}{|\nabla \eta_i - \nabla \eta_j|} \quad (5)$$

the inclination of the boundary between grains with orientations i and j. The parameter m is constant. In general, θ is a vector with 3 independent coordinates, and the $\phi_{i,j}$ are vectors with 2 independent coordinates. At a boundary between grains i and j, $\kappa(\theta, \phi) = \kappa_{i,j}(\phi_{i,j})$, $\gamma(\theta, \phi) = \gamma_{i,j}(\phi_{i,j})$, and $L(\theta, \phi) = L_{i,j}(\phi_{i,j})$, since only η_i and η_j differ from zero. The magnitude and inclination dependence of the grain boundary energy and mobility can thus be specified for $p - 1$ discrete misorientations. Since structural relaxations with respect to misorientation are

not relevant on the mesoscale, the misorientation dependence is treated in a discrete way and considered to be fixed for a given grain configuration [the η-dependence in Eq. (4) is omitted when calculating the driving forces in Eq. (1)]. On the other hand, the model parameters are continuous functions of the inclination, to describe the reorientation of grain boundaries towards a low energy inclination, occurring on the mesoscale.

In [23], we study how the model parameters affect the free energy density f_0 and the shape of the equilibrium phase field profiles across grain boundaries. Furthermore, we derive expressions for the grain boundary energy $\sigma_{gb}(\theta, \phi)$ and mobility $\mu_{gb}(\theta, \phi)$ as a function of the model parameters, giving

$$\sigma_{gb}(\theta, \phi) = g(\gamma(\theta, \phi))\sqrt{\kappa(\theta, \phi)m}, \quad (6)$$

$$\mu_{gb}(\theta, \phi)\sigma_{gb}(\theta, \phi) = \kappa(\theta, \phi)L(\theta, \phi), \quad (7)$$

where $g(\gamma)$ has to be evaluated numerically. We also define a measure ℓ_{gb} for the grain boundary width, which is based on the maximum gradients of the phase fields:

$$\ell_{gb} = \sqrt{\frac{\kappa(\theta, \phi)}{m f_{0,\text{interf}}(\gamma(\theta, \phi))}}. \quad (8)$$

$f_{0,\text{interf}}(\gamma)$ refers to the value of f_0 at the middle of the diffuse region, where the 2 phase fields cross. This quantity can be used as a parameter in criteria for the numerical stability and accuracy of the simulation results. In Fig. 1, numerically evaluated function values for $g(\gamma)$ and $f_{0,\text{interf}}(\gamma)$ are compared with $f_{0,\text{saddle}}(\gamma)$, the value of f_0
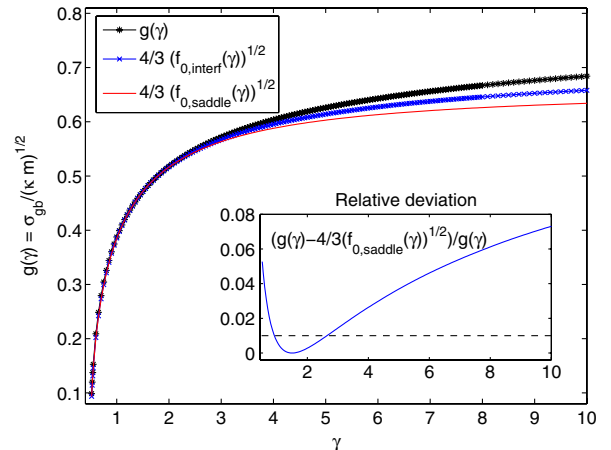

FIG. 1 (color online).   Numerically calculated function values for $g(\gamma) = \sigma_{gb}/\sqrt{\kappa m}$ and $4/3\sqrt{(f_{0,\text{interf}}(\gamma))}$, compared with the analytical function $4/3\sqrt{(f_{0,\text{saddle}}(\gamma))}$, which is the value of f_0 at its saddle point. The relative deviation between $g(\gamma)$ and $4/3\sqrt{(f_{0,\text{saddle}}(\gamma))}$ is also plotted as a function of γ.

at its saddle point, for which an analytical expression exists. It is shown in [23] that for $\gamma = 1.5$, $g(\gamma) = 4/3\sqrt{f_{0,\text{interf}}(\gamma)} = 4/3\sqrt{f_{0,\text{saddle}}(\gamma)}$. In general, however, there is no simple relation between the three functions. The approach of Kazaryan *et al.* [2] is accordingly not quantitative, especially for large variations in grain boundary energy. Using relations (6)–(8), the model parameters can be calculated iteratively for discrete values $\sigma_{\text{gb},k}$ and $\mu_{\text{gb},k}$, and a constant grain boundary width ℓ_{gb}, as described in [23]. To enhance evaluation of the expressions, polynomials $\tilde{g}(\gamma)$ and $\tilde{f}_0(\gamma)$ were fitted through the numerically calculated values for $g(\gamma)$ and $f_0(\gamma)$.

To formulate the inclination dependence, we assume that the grain boundary energy and mobility for different misorientations k have the form $\sigma_{\text{gb},k}(\phi) = \bar{\sigma}_{\text{gb},k}f_{\sigma,k}(\phi)$ and $\mu_{\text{gb},k}(\phi) = \bar{\mu}_{\text{gb},k}f_{\mu,k}(\phi)$, with ϕ measured with respect to the crystal lattice of the adjacent grains. For the model parameters, we take the form

$$\kappa_{i,j}(\phi_{i,j}) = \bar{\kappa}_k f_{\kappa,k}(\phi), \quad (9a)$$

$$\gamma_{i,j}(\phi_{i,j}) = f_{\gamma,k}(\bar{\gamma}_k, \phi), \quad (9b)$$

$$L_{i,j}(\phi_{i,j}) = \bar{L}_k f_{L,k}(\phi), \quad (9c)$$

where k is the misorientation between grains i and j and $\phi_{i,j}$ defined with respect to the system [Eq. (5)] and related to $\phi_{i,j}$ through the orientations i and j. For weak inclination dependence of the grain boundary energy ($\sigma_{\text{gb}} + d^2\sigma_{\text{gb}}/d\phi^2 > 0$, $\forall \phi$), $f_{\kappa,k}(\phi)$ is taken equal to $f_{\sigma,k}(\phi)$, $f_{L,k}(\phi) = f_{\mu,k}(\phi)$ and $f_{\gamma,k}(\bar{\gamma}_k, \phi) = g^{-1}(x)$ with $g^2(\gamma_{i,j}) = g^2(\bar{\gamma}_k)f_{\sigma,k}(\phi)$. Values for m, $\bar{\gamma}_k$, $\bar{\kappa}_k$, and $\bar{L}_k$ are calculated from relations (6)–(8), using the given $\bar{\sigma}_{\text{gb},k}$, $\bar{\mu}_{\text{gb},k}$ and an appropriate ℓ_{gb}. For strong inclination dependence, only a limited number of narrow inclination ranges located around some extrema of the inclination
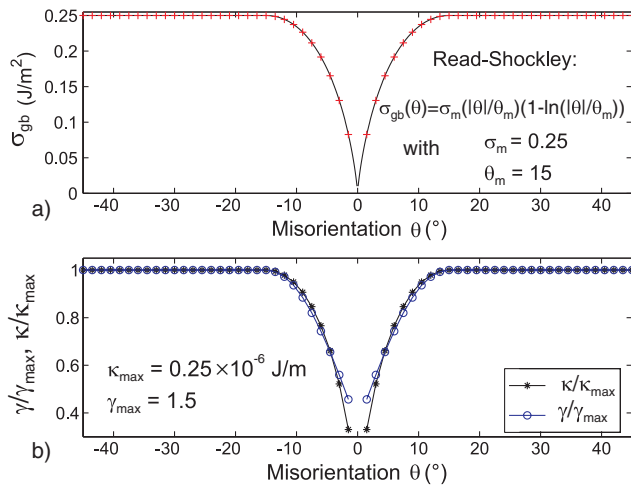

FIG. 2 (color online).   (a) Grain boundary energy as a function of misorientation and (b) the corresponding values for the model parameters κ and γ used for the simulations depicted in Fig. 3.

dependent factors $f_{\sigma,k}(\phi)$ and $f_{\mu,k}(\phi)$ dominate the morphology. Then, it is more convenient to calculate first discrete model parameter values κ_l, γ_l, L_l and m for the grain boundary energies $\sigma_{\text{gb},l}$ and mobilities $\mu_{\text{gb},l}$ at inclinations l for which $f_{\sigma,k}(\phi_k)$ or $f_{\mu,k}(\phi_k)$ are extremal, and fixed ℓ_{gb}. Next, $f_{\gamma,k}(\bar{\gamma}_k, \phi) = \bar{\gamma}_k f'_{\gamma,k}(\phi)$ is taken and $f_{\kappa,k}(\phi)$ and $f_{\gamma,k}(\phi)$ must be functions with cusps and extrema at the same inclinations as $f_{\sigma,k}(\phi)$. Furthermore, $\bar{\kappa}_k$ and $\bar{\gamma}_k$ and the coefficients in $f_{\kappa,k}(\phi)$ and $f_{\gamma,k}(\phi)$ are calculated so that $\bar{\kappa}_k f_{\kappa,k}(\phi_l)$ and $\bar{\gamma}_k f'_{\gamma,k}(\phi_l)$ equal the formerly calculated κ_l and γ_l. A similar approach is applied for the kinetic parameter. Intermediate strengths of inclination dependence may be treated by both approaches.

As a first illustration, we determine the model parameters for a system with Read-Shockley misorientation dependence of the grain boundary energy [12] for low-angle misorientations, and the σ_{gb} constant for high-angle misorientations (see Fig. 2). A fourfold symmetry is assumed. The orientations within one quadrant are discretized with an interspacing of 1.5° and assigned to 60 order parameters. The misorientation between grains with orientations i and j is calculated as $\theta = 1.5°(|j - i|)$ for $|j - i| \leq 30$ or $\theta = -90° + 1.5°(|j - i|)$ for $|j - i| \geq 30$. These simulations are representative for the evolution of a polycrystalline film with fiber texture. The grain boundary mobility is taken constant, $\mu_{\text{gb}} = 1 \times 10^{-6}$ m^2 s/kg, and the grain boundary width is taken $\ell_{\text{gb}} = 1.33 \times 10^{-6}$ m. Calculation of the model parameters gives $m = 2.25 \times 10^6$ J/m^3, $L = 1$ m · s/kg, and values for $\kappa_{i,j}$ and $\gamma_{i,j}$ as shown in Fig. 2. If there are cusps in the grain boundary energy at high-angle misorientations, the same procedure is used to calculate the model parameters. A standard explicit finite difference discretization with grid spacing $\Delta x = 0.2 \times 10^{-6}$ m and time step $\Delta t = 0.03$ s was used for the numerical implementation. The images in Fig. 3 show that the model is able to distinguish between different grain boundary energies and different triple junction angles. Simulations for individual triple junction geometries indicate that the accuracy of the simulations is
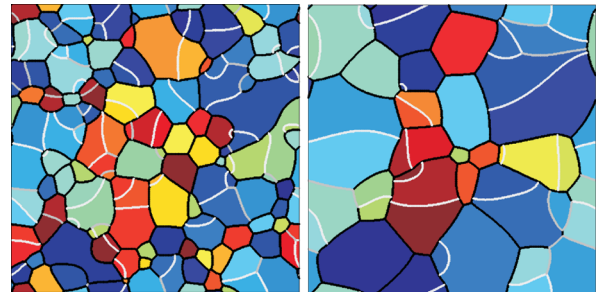

FIG. 3 (color online).   Simulation images at times 202.5 and 892.5 sec, for the conditions specified in the text and in Fig. 2, and a system size 100×100 μm^2. Grain boundaries with misorientation $\pm 1.5°$ are in white, those with misorientation $\pm 3°$ in gray.
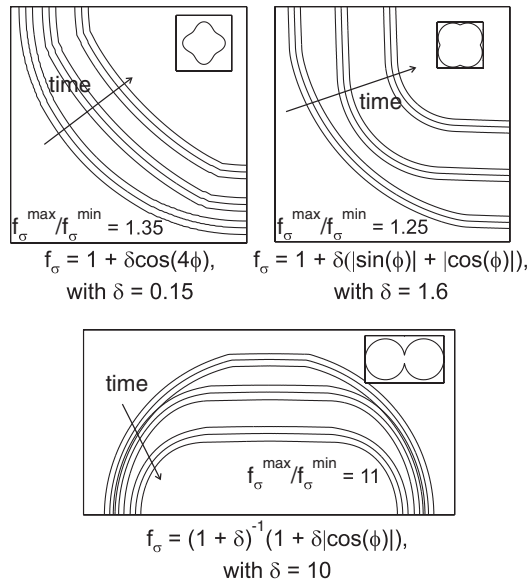
FIG. 4.   Contour lines for $\eta_1 = 0.1$, 0.5, and 0.9 at 3 different time steps, obtained from 2D simulations of a shrinking grain using different inclination dependent factors [24–26] for the grain boundary energy. The polar plot of the grain boundary energy is also shown. The simulations are for $\bar{\sigma}_{gb} = 0.25$ J/m^2, $\mu_{gb} = 1 \times 10^{-6}$ m^2 s/kg, $\ell_{gb} = 1.33 \times 10^{-6}$ m, $\Delta x = 0.1 \times 10^{-6}$ m, $\Delta t = 0.002$ s, and system size 50×50 μm^2.

controlled by $\ell_{gb}/\Delta x$ (for $\ell_{gb} < 5R$) [23]. Moreover, larger variations in grain boundary energy require a higher resolution for the same accuracy. For $\ell_{gb}/\Delta x = 6.65$, the error on the grain boundary curvatures is below 2% for junctions with all angles between approximately 110° and 130°, below 5% when angles are between 90° and 140°, and between 5% and 10% if 1 of the angles is between 75° and 90° or between 140° and 143°. For $\ell_{gb}/\Delta x = 13.3$, the error is reduced with 1%–3% for the two latter situations. For Read-Shockley misorientation dependence, a finer discretization of the grain orientations is thus only useful if $\ell_{gb}/\Delta x$ is increased as well. A similar resolution dependent restriction was observed for Monte Carlo simulations [11]; however, the phase-field method gives more flexibility to improve the numerical resolution in an efficient way, also in 3D, e.g., by a thin-interface approach, adaptive meshing and sparse data structures.

As a second illustration, we simulate the curvature driven shrinkage of an initially circular grain, using grain boundary energies with different inclination dependence. The contour lines at different values of the phase field, representing the shrinking grain in Fig. 4, show that the grain boundary width is indeed constant.

To conclude, we have introduced a modified phase-field model, and a procedure to determine its model parameters, for grain growth. The methodology allows us to account correctly for grain boundary mobility and stiffness data, for example, obtained from molecular dynamics simulations,

in mesoscale simulations, and gives high controllability of the numerical accuracy.

*Nele.Moelans@mtm.kuleuven.be

[1] D. Fan and L.-Q. Chen, Acta Mater. **45**, 611 (1997).
[2] A. Kazarayan, Y. Wang, S. Dregia, and B. Patton, Acta Mater. **50**, 2491 (2002).
[3] N. Moelans, B. Blanpain, and P. Wollants, Acta Mater. **55**, 2173 (2007).
[4] C. E. Krill III and L.-Q. Chen, Acta Mater. **50**, 3057 (2002).
[5] S. Kim, D. Kim, W. Kim, and Y. Park, Phys. Rev. E **74**, 061605 (2006).
[6] Y. Suwa, Y. Saito, and H. Onodera, Comput. Mater. Sci. **40**, 40 (2007).
[7] M. Upmanyu, G. Hassold, A. Kazaryan, E. Holm, Y. Wang, B. Patton, and D. Srolovitz, Interface Sci. **10**, 201 (2002).
[8] K. Janssens, D. Olmstead, E. A. Holm, S. Foiles, S. Plimpton, and P. Derlet, Nat. Mater. **5**, 124 (2006).
[9] S. Foiles and J. Hoyt, Acta Mater. **54**, 3351 (2006).
[10] F. Humphreys, Acta Mater. **45**, 4231 (1997).
[11] E. Holm, M. Miodownik, and A. Rollett, Acta Mater. **51**, 2701 (2003).
[12] F. J. Humphreys and M. Hatherly, *Recrystallization and Related Annealing Phenomena* (Pergamon, Oxford, 1996).
[13] J. A. Warren, R. Kobayashi, E. Lobkovsky, and W. C. Carter, Acta Mater. **51**, 6035 (2003).
[14] T. Pusztai, G. Bortel, and L. Gránásy, Europhys. Lett. **71**, 131 (2005).
[15] L. Gránásy, T. Pusztai, T. Börzsönyi, G. Tóth, and G. Tegze, J. Mater. Res. **21**, 309 (2006).
[16] M. Tang, W. Carter, and R. Cannon, Phys. Rev. B **73**, 024102 (2006).
[17] J. Mellentin, M. Plapp, and H. Henry (to be published).
[18] I. Steinbach, F. Pezzolla, B. Nestler, M. Seeßelber, R. Prieler, G. J. Schmitz, and J. L. L. Rezende, Physica (Amsterdam) **94D**, 135 (1996).
[19] H. Garcke, B. Nestler, and B. Stoth, SIAM J. Appl. Math. **60**, 295 (1999).
[20] B. Echebarria, R. Folch, A. Karma, and M. Plapp, Phys. Rev. E **70**, 061604 (2004).
[21] A. Kazaryan, Y. Wang, S. Dregia, and B. Patton, Phys. Rev. B **63**, 184102 (2001).
[22] N. Ma, Q. Chen, and Y. Wang, Scr. Mater. **54**, 1919 (2006).
[23] N. Moelans, B. Blanpain, and P. Wollants, Phys. Rev. B (to be published).
[24] J. Eggleston, G. McFadden, and P. Voorhees, Physica (Amsterdam) **150D**, 91 (2001).
[25] J. Debierre, A. Karma, F. Celestini, and R. Guerin, Phys. Rev. E **68**, 041604 (2003).
[26] I. Loginova, J. Agren, and G. Amberg, Acta Mater. **52**, 4055 (2004).